SEGMENTATION BY DEFORMABLE CONTOURS OF MRI SEQUENCES OF THE LEFT VENTRICLE FOR QUANTITATIVE ANALYSIS

D Richens*, N Rougon*, I Bloch*, E Mousseaux**

*Télécom Paris, France; ** Hôpital Broussais, France

1 INTRODUCTION

Certain Magnetic Resonance Imaging (MRI) techniques, such as *gradient-echo*, allow for rapid acquisition speeds suitable for acquiring motion picture studies of the heart over a whole cardiac cycle. This gives cardiologists another tool for detecting and assessing pathologies of the heart. For the most part cardiologists are more interested in the performance of the left ventricle (LV), as it is a powerful blood pump for the systemic circulation. As an imaging modality, MRI systematically provides excellent blood/tissue/air contrast regardless of the subject's condition, while remaining completely non-invasive. Unlike cardiac angiography, perhaps the currently favored technique for quantitative cardiac analysis, the epicardium is rendered as well as the endocardium. Echocardiography, though allowing to visualize both of these structures, produces noisy images and is highly sensitive to variation between patients, especially because of frequently occuring air pockets which obscure important features.

However, manual measurement of MRI data is time consuming and provides results that are essentially non-reproducible. This is especially true for volume measurements that require a cardiologist to delineate the contour of the body to be measured. As it is apparent that quantitative measurements from 3-D medical imagery can be very useful, much work has been done in order to reduce or eliminate the need for human involvement in the measuring process. In particular Fleagle *et al.* [2] use a graph technique for finding the epicardium and endocardium from MRI images, and Lilly *et al.* [4] use *knowledge-based cost functions* to extract borders from cineangiographic images segmented by thresholding the image gradients.

In this article, we present an application of a deformable contour model to extract the epicardial and endocardial boundaries of the LV from a time sequence of cardiac MR Images. The deformable model that we use is based on the work of Rougon and Prêteux [6]. In order to exploit both the geometric and photometric information present in temporal image sequences, an additional coupling force between the contours located in adjacent images is introduced. Automatic and robust initialization procedures for the iterative optimization of the model are investigated in order to reduce interactivity. The segmentation results are then used to calculate the evolution of the LV volume during the cardiac cycle. From these measurements, it is possible to compute precisely clinical parameters such as peak filling rate or ejection fraction. This method provides therefore a first step towards an automatic quantitative characterization of heart function.

2 IMAGE SEGMENTATION BY ACTIVE CONTOURS

In this section, we discuss the process used in going from raw data to the computation of our quantitative parameters. The raw image data come from two centers: 1) a 1.5T Signa (General Electric) with an echo delay TE = 17 ms, a repetition time TR = 31 ms, a flip angle = 30° and a slice thickness of 10 mm, 2) a 1.5T Gyroscan (Philips) with a TE = 13 ms, TR = 25 ms, flip angle = 45° and a slice thickness of 8 mm. For both machines, the image matrix consists of 128 lines of 256 pixels, reconstructed as a matrix of 256 lines of 256 pixels. Acquisitions were gated on the R wave of the ECG and averaged over two measurements per slice. Therefore, the number of frames per cardiac cycle depends on the heart rate and on the number of TR times that could be fitted into the RR interval. This results in anywhere from 19 to 27 images per cardiac cycle, depending on the subject's heart rate. The field of view provides a spatial resolution from 1.44 mm to 1.56 mm per pixel.

2.1 Active contours for segmentation

The segmentation is achieved using an active contour model called *g-snake* [6] which extends the classical *snake* model [3, 1]. This method was chosen since it has been shown to work efficiently on images where noise renders useless edge detection relying on discrete differential operators.

Briefly, the segmentation is performed by iteratively deforming an initial approximation $\mathcal{C}^0$ of the contour to be determined. In g-snake modelling, contours are described as closed almost-everywhere $\mathcal{C}^2$-continuous curves which behave as expanding/contracting inhomogeneous membrane/thin-plates. Therefore, the contour delineates a controlable area while resisting to stretching and bending. These mechanical properties are specified by an internal energy expressed by :

$$E_{int}(\mathcal{C}) = \int_0^1 \alpha(s)\|\vec{X}_s\|^2\,ds + \int_0^1 \beta(s)\|\vec{X}_{ss}\|^2\,ds - \int_0^1 \kappa \det(\vec{X}, \vec{X}_s)\,ds \quad , \qquad (1)$$

where $\vec{X}(s) = (x(s), y(s))^T$ denotes the set of points that make up the deformable curve $\mathcal{C}$ parameterized by an arc-length s, $\vec{X}_s \equiv \frac{\partial \vec{X}}{\partial s}$ and $\vec{X}_{ss} \equiv \frac{\partial^2 \vec{X}}{\partial s^2}$. The first two integral terms in (1) refer to the *snake* model [3], and respectively approximate the stretching and bending energy of our membrane/thin-plate model. The term $\beta(s)$ is usually held constant for all points on $\mathcal{C}$, thereby controlling the curvature and limiting the amount of bending. However, we let

the $\alpha(s)$ term be determined separately for each point on $\mathcal{C}$ by the local curvature of the contour. This is done in order to avoid problems at points with high curvature where too much stretching of the contour can cause a discontinuity. Other adaptivity schemes for material properties can be found in [8]. The third integral term in (1) is an isotropic pressure potential which controls the evolution of the area $\mathcal{A}(\mathcal{C}) = \frac{1}{2}\int_0^1 \det(\vec{X}, \vec{X}_s)\, ds$ of the region limited by $\mathcal{C}$. The term $\kappa \in \mathbb{R}$ determines whether the area is encouraged to increase or decrease, depending on its sign and the orientation of $\mathcal{C}^0$, by pushing or pulling on the contour in the direction normal to the curve.

This contour is deformed to the image contour by applying an external energy potential derived from image data and expressed by:

$$E_{ext}(\mathcal{C}, I) = -\lambda \int_0^1 \|\nabla I(\vec{X})\|^2 \, ds \quad , \qquad (2)$$

where $\|\nabla I(\vec{X})\|$ denotes the magnitude of the image gradient, and $\lambda > 0$ is a weighting coefficient. Gradients were evaluated using a recursive implementation of the Difference of Gaussian operator. The standard deviation of the gaussian filter is set to half a pixel, as MRI images generally don't suffer from that much additive noise of the "salt and pepper" type.

The segmentation is found by iteratively minimizing the total energy of the system defined as the sum of E_{int} and E_{ext}. A complete description of the discrete model and the deformation process can be found in [6].

2.2 Coupled active contours [7]

We now present a modification to the *g-snake* model which aims to explicitely exploit the sequential nature of our image sets. For instance, images taken from the diastasis stage of ventricular filling can often provide a weaker signal from the inside of the ventricle due to the lower blood flow, hence making the endocardial border less prominent. If the image just before and the image just after have a reasonable strong signal, however, we can use the positions of the active contours of these two images to guide the contour of the weak image.

In this case, we need to consider our set of images as mappings on a Euclidean 3-space $\mathcal{E}_3$, when the 3$^{\text{rd}}$ dimension is temporal. More precisely, given a sequence of N images, let $(\Pi_i)_{i\in[1..N]} \subset \mathcal{E}_3$ denote a set of Euclidean planes defined, respectively, by equations $z = z_i, z_i \in \mathbb{R}$, so that Π_i is the support space for image i. In each image i, we can then define an active contour $\mathcal{C}_i$ as a set of points $\vec{X}(s) = (x(s), y(s), z(s) = z_i)$ of Π_i together with internal and external energy functionals E^i_{int} and E^i_{ext}, respectively. The expression for the total energy of all of the active contours is given by:

$$E_{tot} = \sum_{i=1}^{N} E^i_{int} + \sum_{i=1}^{N} E^i_{ext} + 2\sum_{i=1}^{N}\sum_{j=i+1}^{N} E^{i,j}_{cpl} \quad , \qquad (3)$$

where $E^{i,j}_{cpl}$ is the energy resulting from the addition of a coupling force between the contours, defined as:

$$\left.\begin{array}{c} \forall (i,j) \in [1..N]^2 \, , \\ E^{i,j}_{cpl} = \displaystyle\int_0^1 \rho \cdot \|\vec{X}^i - \vec{X}^j\|^2 - (z_i - z_j)^2 \, ds \\ \text{iff } (i-j=1) \vee (i=1, j=N) \end{array}\right\} \quad , \qquad (4)$$

otherwise $E^{i,j}_{cpl}$ equals zero. When $i - j = 1$ we are coupling an image contour with those of its two immediate neighbours. Since our image sequences are looped, we are also coupling the contours of the first ($i = 1$) and the last images ($j = N$). The non-negative parameter ρ determines the extent of the coupling force with respect to all the other forces acting on the contours.

Extending the deformation process given in [6] is relatively straightforward and is performed by defining the coupling force as an additional external force.

Ideally, the iterative process is said to have converged when none of the points along the contour move between two successive iterations. However, this requires substantial computation, hence in practice, we considered the process to have converged when $|E^{(t)}_{tot} - E^{(t-1)}_{tot}| < \varepsilon$, where $\varepsilon > 0$ is experimentaly determined.

2.3 Initialization by morphological methods

Our MRI images contain two continuous edges of interest: the epicardial border and the endocardial border. Determining which of these two borders is found by our deformation process depends somewhat on our selection of the parameters describing the deformable contours and the deformation process. Moreover, in order to improve the robustness of the method while reducing intra- and inter-observer variability, an automatic determination of the initial contour $\mathcal{C}^0$ is necessary. We perform this initialization step by means of mathematical morphology techniques.

As blood generates the strongest signal in *gradient-echo* images, the LV appears in the original images as a bright disc of non-uniform intensity. Therefore, an approximate localization of the LV can be obtained by extracting regional maxima in a filtered version of the original images. The filtering step consists in an opening with a dodecagonal structuring element whose radius is roughly the radius of the interior of the LV. In each image, the initial contour for the endocardial border is positioned on the boundary of the selected maximum. Dilating the initial contour for the endocardium at diastole provides a suitable initialization for finding the epicardial border throughout the cardiac cycle for our set of sequences.

3 QUANTITATIVE STUDY OF THE LEFT VENTRICLE

Volume measurements from temporal sequences of images can be very valuable as they allow for the calculation of parameters of clinical interest such as the *Peak Filling Rate* (PFR), the *Time to Peak Filling Rate* (TPFR), and the *Ejection Fraction* (EF), the definitions of which are given below. These measurements can be calculated either globally for the entire LV, or regionally by dividing the LV into radial sectors and performing the calculations separately for each sector. Given a slice, real volumes are accurately computed by multiplying the voxel size (pixel size $\times$ slice thickness) by the number of pixels in the region delineated by the contours obtained previously, including boundary points.

The EF parameter provides an usual estimation of the LV function. It is computed by the following equation as percentage of end diastolic volume:

$$\text{EF} = \frac{V_{ed} - V_{es}}{V_{ed}} \times 100\,\% \quad , \qquad (5)$$

where V_{ed} and V_{es} are the end diastolic and end systolic volumes, respectively. Dividing the difference by the volume at diastole normalizes the value between patients. The PFR, expressed in milliliters per second, measures the maximum blood flow during the *Rapid Filling Phase* (RFP) of diastole. It is taken from volume curve as the maximum positive slope. To account for variations in heart rate, the slope is normalized by dividing the value by the cardiac frequency, and, as with the EF, the value is normalized with respect to end diastolic volume. This gives us a unitless parameter which indicates the PFR of the heart in end diastolic volumes per duration of the cardiac cycle. The TPFR is the measure of the time from the end of systole to the time of PFR. This measurement indicates the duration of the RFP. Like the PFR, the TPFR should be normalized with respect to the cardiac frequency, so as to indicate the fraction of the entire cardiac cycle occupied by the RFP.

Computing the PFR and TPFR requires the determination of the maximum positive slope point of the volume curve. Data sparseness together with potential outliers along this curve make direct differentiation using first order differences quite unreliable. For instance, for a ventricular radius of ten pixels (typically end systole), a half-a-pixel accuracy on the actual radius leads to a ten percent uncertainty on the volume. An analytical representation of the discrete curve allows, however, to obtain more stable estimates. A satisfactory solution consists in using Discrete Fourier Transform (DFT). Retaining only the first four harmonics in the DFT expansion before performing the inverse transform allows to filter out noisy data. Figure 2 shows the result of the volume fit.

The way in which we divide up the LV for regional measurement is designed to focus on the performance of different sectors of the myocardium. The interior of the LV is divided into radial sectors where measurements are performed individually. The center of such a partition must be a relatively stable point with respect to the heart. Using the centroid of the endocardial border would defeat the purpose of doing the regional measurements. For instance, in the case of a myocardial infarction, the endocardial border next to the dead muscle tissue would move very little during the cardiac cycle. Therefore, the centroid would always be halfway between that point and the endocardial border opposite, leading to nearly identical measurement sets. Hence the centroid of the epicardium must be used. To illustrate this, we have calculated the EF, PFR and TPFR for each radial segment using both the epicardial and the endocardial centroids. Table 1 shows the means and standard deviations for each of these parameters over the six segments.

	endo-centered			epi-centered		
	EF%	PFR	TPFR	EF%	PFR	TPFR
μ	71	3.63	.151	78	4.14	.101
σ	2.5	.456	.0247	20	.963	.0645

Table 1: Means (μ) and standard deviation (σ) of regional measurements taken from the 'exercise' sequence, using the centroid of the *endocardium* and then the *epicardium* as the center of the heart. Note the difference in σ for the EF parameter.

4 RESULTS AND DISCUSSION

Our results are presented in the form of volume curves, and as both global and regional clinical parameters (EF, PFR, TPFR), within a specific slice of the heart. These parameters are intended to indicate the relative performance of the subject's heart and to detect global abnormalities of the LV function in homogeneous diseases, such as hypertension or primitve cardiomyopathies. Furthermore, a segmental analysis could detect regional abnormalities which occur in ischemic disease or asymmetric LV hypertrophy.

We have applied this method to the segmentation of three sets of sequences acquired on three patients at different heart levels and under different cardiac activity conditions. The first data set consists of temporal sequences taken on a patient at rest through the base, the middle and the apex of the LV, respectively. The second set was acquired at the mid-ventricle level before and after an exercise period. Finally, robustness with respect to noise was tested on a degraded sequence acquired at mid-ventricle level on a patient at rest. Table 2 summarizes the results obtained for the EF, PFR and TPFR.

image set	EF	PFR/EDV	PFR_n	$TPFR_n$
base	25	1.03	0.86	.183
mid	59	1.90	1.61	.203
apex	67	3.22	2.68	.194
rested	59	2.86	2.29	.154
exercise	70	5.31	3.75	.146
noisy	35	1.49	1.08	.149

Table 2: Parameters calculated from six image sequences. PFR_n and $TPFR_n$ are normalized as described in the text, PFR/EDV is normalized with respect to End Diastolic Volume (EDV) only, as described in [5].

Figure 2 shows the results of a comparison between the volume measurements made by our method of the 'base', 'mid' and 'apex' sequences, with the volume measurements performed by a cardiologist from manually delineated contours. The slope of the line of best fit is less than one, indicating that the manually derived volumes are generally greater than those derived from the computer generated borders. Manually derived volumes were less for smaller volumes, as shown by the line's intersect of the y-axis. The correlation between the two sets of volumes is $R = 0.995$. Therefore, the discrepancy between the manually and computer derived volumes seems to be systematic. We believe that several causes may help to explain this bias. First, visual effects due to contrast sensitivity of the human eye induce significant changes in the way of positioning the contours. Therefore, the dynamics corrections which the cardiologist intuitively performs when visualizing the images and the low dynamics around gradient maxima must be taken into account. Secondly, because of heart movements, acquisition levels cannot be kept constant with respect to an anatomical coordinate system, so that LV papillary muscle may intersect the slice for some images in the sequence. This spurious effect, which frequently occurs for mid-ventricle slices, is smoothed out by the cardiologist but cannot be handled by our method without including extra anatomical knowledge. Finally, the α and κ parameters should perhaps be altered to allow the contour to expand more. The ECG provides then biologically consistent information to control

the mechanical properties of the curve.

The global results we obtain are the same as those obtained currently with cardiac angiography and with Computed Tomography [5]. In particular, several studies in angiography found the PFR values for rested subjects to be around three EDV/second. Given that their uncertainty was about plus or minus one EDV/second, this agrees with the PFR/EDV from the images taken through the apex, and with the images taken of our 'rested' subject, though the plane of view for the 'rested' set of images was mid-ventricular. Unfortunately, since all subjects for our set of sequences were suffering from some pathology of the heart, it is impossible to make any definite claim.

To conclude, we have presented an original, accurate, semi-automatic and reproducible method to segment MRI cardiac images, allowing to quantify significant clinical parameters. The results that we have obtained have proved to be similar to those obtained by physicians in a manual, non reproducible fashion[2]. Future developments will deal with improving the robustness of the initialization step and devising adaptivity schemes for parameters tuning, as well as beginning a cautious clinical validation on larger data sets including both normal and pathological subjects.

REFERENCES

[1] Cohen LD, March 1991, "Note On Active Contour Models and Balloons", Computer Vision, Graphics and Image Processing, 53(2), 211–218.

[2] Fleagle SR, Thedens DR, Ehrhardt JC, Scholz TD, Skorton DJ, April 1991, "Automated Identification of Left Ventricular Borders from Spin-Echo Magnetic Resonance Images; Experimental and Clinical Feasibility Studies", Investigative Radiology, 26(4), 295–303.

[3] Kass M, Witkin A, Terzopoulos D, 1988, "Snakes: Active Contour Models", Int. Journal Computer Vision, 1(4), 321–331.

[4] Lilly P, Jenkins J, Bourdillon P, June 1989, "Automatic Contour Definition on Left Ventriculograms by Image Evidence and a Multiple Template-Based Model", IEEE Trans. Medical Imaging, 8(2), 173–185.

[5] Ollivier JP, December 1990, "Valeur des méthodes non invasives d'exploration du remplissage du ventricule gauche", Réalités Cardiologiques, 10, 13–20.

[6] Rougon N, Prêteux F, July 1991, "Deformable Markers: Mathematical Morphology for Active Contour Models Control", Proc. SPIE 1991 International Symposium on Optical Applied Science and Engineering, 1610, San Diego, California, 78–89.

[7] Rougon N, November 1991, "Deformable markers for segmentation", Internal Report Télécom Paris Département Images.

[8] Samadani R, July 1991, "Adaptive Snakes: Control of Damping and Material Parameters", Proc. SPIE's 1991 International Symposium on Optical Applied Science and Engineering – Geometric Methods in Computer Vision, 1570, San Diego, California.

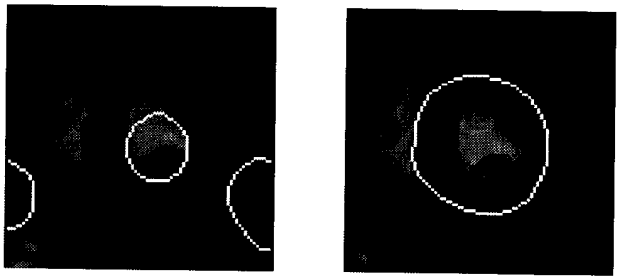

Figure 1: Contours of the regional maxima of the morphologically filtered image *(left)*. We assume that the contour found around the center point of the image is the C^0. Final endocardial and epicardial contours *(right)*.

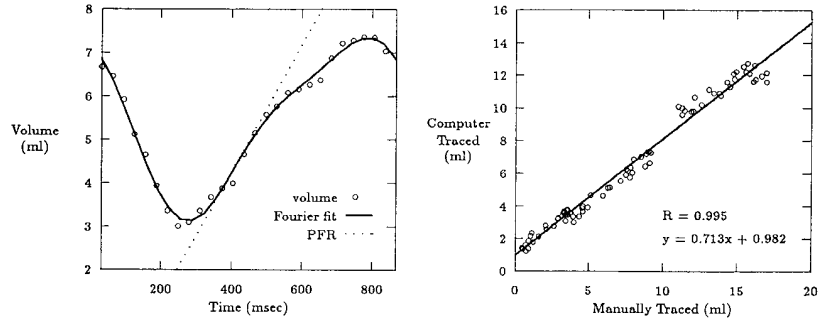

Figure 2: *Left:* The result of fitting the volume data with fourier series. Line tangent to the curve indicates the maximum slope of the function, used to calculate the PFR. *Right:* Comparison of volumes calculated from computer derived endocardial borders with those calculated from manually traced borders. Correlation between the two sets of measurements is R = 0.995.